INSTITUTE OF PHYSICS PUBLISHING JOURNAL OF PHYSICS: CONDENSED MATTER

J. Phys.: Condens. Matter **15** (2003) 7385–7394 PII: S0953-8984(03)65192-1

Structure and magnetic transition of $LaFe_{13-x}Si_x$ compounds

Xu Bo Liu, Z Altounian[1] and D H Ryan

Centre for the Physics of Materials and Department of Physics, McGill University, Rutherford Physics Building, 3600 University Street, Montreal, Quebec, H3A 2T8, Canada

E-mail: zaven@physics.mcgill.ca

Received 21 June 2003
Published 17 October 2003
Online at stacks.iop.org/JPhysCM/15/7385

Abstract

Structure and magnetic transitions were investigated by x-ray diffraction and Mössbauer spectroscopy in $LaFe_{13-x}Si_x$ compounds with $x = 1.6$, 2.0 and 2.6. With increasing Si content, the La–Fe interatomic distance decreased while the average Fe–Fe distance increased. These changes affect the structural stability and the magnetic properties of the compounds. The temperature dependence of the hyperfine field for the compound with $x = 2.6$ can be fitted very well using a mean field model with a Brillouin function (BF) while that for the compounds with $x = 1.6$ and 2.0 changes more sharply than that predicted by the BF relation near the Curie temperature. The different nature of the magnetic transition with different Si content originates from the spatial distribution of the Si atoms and related variation of the La–(Fe, Si) and the Fe–Fe distances in the cubic $NaZn_{13}$ structure.

1. Introduction

Recently, research interest on the giant magnetocaloric effect (MCE) at room temperature has been considerably enhanced. It is reported that the compounds of $Gd_5Si_2Ge_2$ [1], $La_{1-x}Ca_xMnO_3$ [2], $LaFe_{11.4}Si_{1.6}$ [3] and $MnFeP_{1-x}As_x$ [4] exhibit considerable MCE due to a first order ferromagnetic to paramagnetic (F–P) transition near the Curie temperature, T_C.

$LaFe_{13-x}Si_x$ compounds have a cubic $NaZn_{13}$ structure with the space group $Fm\bar{3}c$ and a ferromagnetic ground state when $1.3 \leqslant x \leqslant 2.6$ [5]. It has been found that $LaFe_{11.4}Si_{1.6}$ exhibits a giant MCE and shows a large magnetic entropy change, $|\Delta S| = 19.4\ \mathrm{J\ kg^{-1}\ K^{-1}}$ at $T_C = 208$ K [3]. With increasing Si content, T_C increases, but the magnetic entropy change decreases rapidly [6]. It is believed that the nature of magnetic transition near T_C changes from first order to second order. However, there is no report on why the order of magnetic transition changes with Si content in $LaFe_{13-x}Si_x$ compounds. In this paper, we investigate

[1] Author to whom any correspondence should be addressed.

the relationship between the structure and the magnetic transition near T_C in $LaFe_{13-x}Si_x$ compounds. Our Mössbauer results clearly show the magnetic transition changes gradually from strongly first order to weakly first order and second order for $x = 1.6$, 2.0 and 2.6. Powder x-ray diffraction (XRD) and Wigner–Seitz cell calculations indicate the average Fe–Fe distances increase with increasing Si content, which changes the order of the magnetic transition in $LaFe_{13-x}Si_x$ compounds.

2. Experimental techniques

Alloys with nominal composition of $LaFe_{13-x}Si_x$ ($x = 1.6, 2.0, 2.6$) were prepared in purified Ar atmosphere by a tri-arc melting method. The ingots were annealed at 1273 K for 15 days in evacuated quartz tubes. The x-ray powder diffraction analysis were performed on an automated Nicolet x-ray powder diffractometer with Cu Kα radiation. The diffractometer has a Bragg–Brentano geometry and a graphite monochromator in the diffracted beam. The data analysis was carried out using *Fullprof* computer codes based on the Rietveld powder diffraction profile fitting technique [7, 8]. The Curie temperatures were determined by AC susceptibility (χ_{ac}), using a quantum design physical property measurement system (PPMS) magnetometer.

The Mössbauer spectra for $LaFe_{13-x}Si_x$ samples were obtained in a standard transmission geometry with a 1 GBq ^{57}Co**Rh** source on a constant acceleration spectrometer, which was calibrated against an α-iron foil at room temperature. A liquid nitrogen flow cryostat was used to obtain temperatures between 100 and 300 K. Spectra were fitted using a standard nonlinear least-squares minimization method.

3. Results and discussion

3.1. Crystal structure

Figure 1 displays the XRD patterns and Rietveld refinements for $LaFe_{13-x}Si_x$ compounds with $x = 1.6$, 2.0 and 2.6. All samples show a main phase with the cubic $NaZn_{13}$ structure (space group: $Fm\bar{3}c$). The diffraction peaks shift to high angle with increasing Si content, indicating the reduction of the unit cell. In $LaFe_{13-x}Si_x$ compounds, the La, 8a and Fe_1, 8b sites are fixed at (1/4, 1/4, 1/4) and (0, 0, 0), respectively. The fractional coordinates for the Fe_2, 96i sites are ($0, y, z$). The slight variations in the relative x-ray peak intensities (figure 1) are caused by the different Si contents and the slight changes in the fractional coordinates of the Fe_2, 96i sites.

In the La–Fe–Si ternary system, as shown below, the chemical affinity for La–Si is very strong and that for Fe–Si is moderate. The enthalpy of mixing for La–Fe is positive, which means no formation of binary La–Fe phase. In the $LaFe_{13-x}Si_x$ alloys, the most possible impurity is La–Si phase and α-Fe. In fact, for the sample with $x = 1.6$ (figure 1(a)), there are two weak Bragg peaks at 23.1° and 32.8°, which could originate from some La–Si phase. The most likely La–Si phase is $LaSi_2$ with the $GdSi_2$ structure (space group: $Pmma$, $a = 4.27$ Å, $b = 4.17$ Å and $c = 14.05$ Å [9]). This phase has its strongest peak at 32.6° and two medium strength peaks at about 21.9° and 22.4°. Similarly, the sample with $x = 2.0$ has a weak Bragg peak at 33° (figure 1(b)). For $x = 2.6$, the alloy crystallizes in a single phase with the $NaZn_{13}$ structure (figure 1(c)). The appearance of La–Si phases induce the formation of some α-Fe in the alloys. Although no visible Bragg peaks of α-Fe are seen in the XRD patterns for $x = 1.6$ and 2.0, the Mössbauer spectra, shown below, indicate there is a small amount (<4%) of α-Fe in the sample with $x = 1.6$ and 2.0.

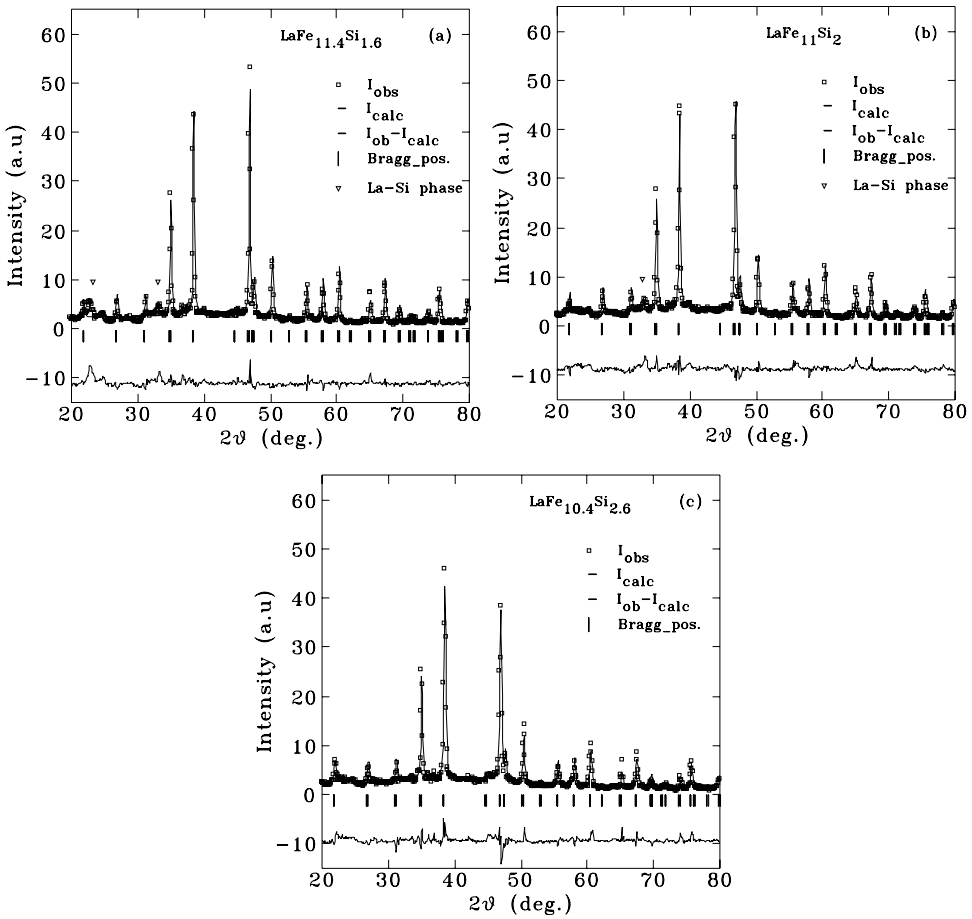

Figure 1. Rietveld fitted XRD patterns for $LaFe_{13-x}Si_x$ compounds. (a) $x = 1.6$, (b) $x = 2.0$ and (c) $x = 2.6$.

It should be noted that the region related to the peaks of the La–Si phases for $x = 1.6$ and 2.0 is excluded in the Rietveld refinement process because the peaks are too few to refine the La–Si phase. The refinement results are also listed in table 1. The lattice constant, a, decreases and the atomic position of Fe_2 changes with increasing Si content. The Si atoms only enter the 96i sites and the Fe and Si atoms are randomly distributed at the Fe_2 positions, which is in agreement with [10]. As given below, those structural changes have a critical effect on the stability and the magnetic properties of these compounds.

3.2. Magnetic properties

Figure 2 displays the temperature dependence of the AC magnetic susceptibility, χ, for $LaFe_{13-x}Si_x$ compounds. With increasing Si content, T_C increases and the AC magnetic susceptibility change becomes less abrupt near T_C.

Temperature dependent ^{57}Fe Mössbauer spectra for the three samples have been measured in the temperature range $100\ \mathrm{K} \leqslant T \leqslant 300\ \mathrm{K}$. The Mössbauer spectra at different temperature around their T_C for $LaFe_{13-x}Si_x$ with $x = 1.6$, 2.0 and 2.6 are shown in figure 3. The

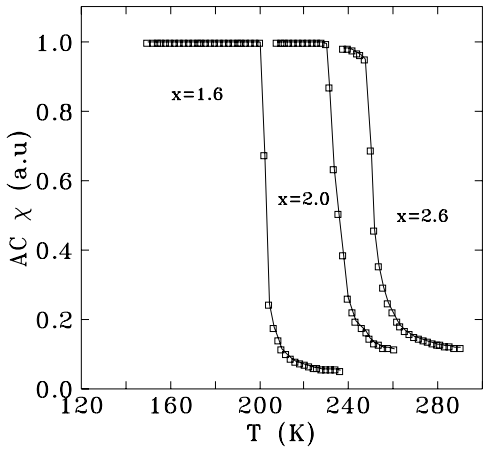

Figure 2. Temperature dependence of the AC magnetic susceptibility, χ, for $LaFe_{13-x}Si_x$ compounds.

Table 1. Lattice parameter and the fractional coordinates of Fe_2 96i sites for $LaFe_{13-x}Si_x$ compounds deduced by a Rietveld powder diffraction profile-fitting technique.

	x		
	1.6	2.0	2.6
a (Å)	11.465(1)	11.461(1)	11.443(1)
x	0	0	0
y	0.1783(3)	0.1790(1)	0.1802(2)
z	0.1167(1)	0.1168(1)	0.1193(3)

temperature dependence of hyperfine field for the compounds is displayed in figure 4. The spectra for $LaFe_{11.4}Si_{1.6}$ and $LaFe_{11}Si_2$ have a very small subspectrum corresponding to α-Fe (<4 at%). The formation of α-Fe is related to the appearance of the La–Si phases as discussed above.

In addition to a very small subspectrum corresponding to α-Fe, the spectrum for $LaFe_{11.4}Si_{1.6}$ is dominated by a Gaussian magnetic sextet at temperatures, $T \leqslant 200$ K (figure 3(a)). With increasing temperature, the average hyperfine field, $B_{\rm hf}(T)$, of the sextet decreases. However, in addition to the sextet corresponding to a magnetically ordered state, there is an asymmetric doublet indicating a paramagnetic state at 202 and 205 K. The coexistence of the ferromagnetic and paramagnetic states is due to the superheating effect and is an indication of a first order transition. At 215 K, the average hyperfine field $B_{\rm hf}$ decreases to zero and the sextet component is totally replaced by the doublet, indicating that the compound is in a paramagnetic state.

The Mössbauer spectra for the $LaFe_{10.4}Si_{2.6}$ compound change slowly to an asymmetric spectrum characteristic of a paramagnetic state at $T_{\rm C}$ from a Gaussian sextet of a magnetically ordered state with increasing temperature (figure 3(c)). An asymmetric doublet appears and completely replaces the magnetic sextet at 250 K. There is no sign of the coexistence of the magnetic sextet and paramagnetic doublet. Similarly, the Mössbauer spectra for $LaFe_{11}Si_2$ change slowly from ferromagnetic sextet to paramagnetic doublet and no sign of the coexistence of the ferromagnetic and paramagnetic components.

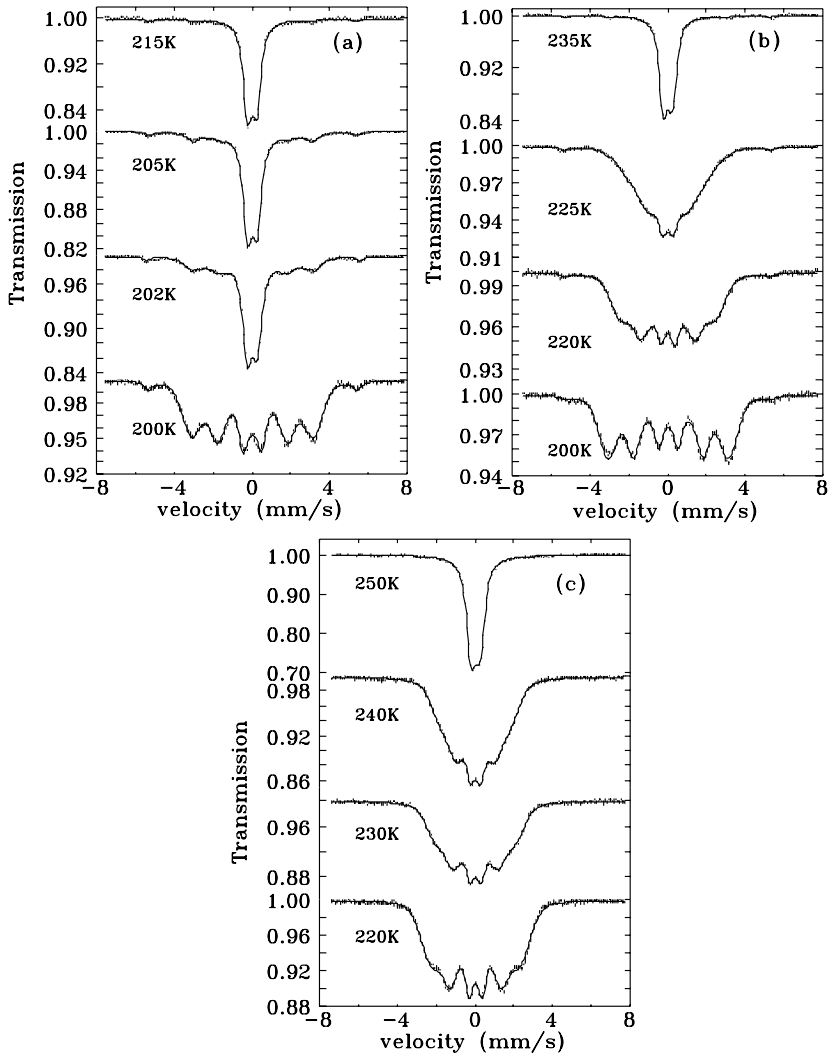

Figure 3. ^{57}Mössbauer spectra of $LaFe_{13-x}Si_x$ compounds at several temperatures. (a) $x = 1.6$, (b) $x = 2.0$ and (c) $x = 2.6$. The solid curves are least squares fits to the Mössbauer spectra.

There is an approximately linear correlation between the mean hyperfine field, $B_{\rm hf}(T)$, and the mean magnetic moment. The reduced magnetization, $m = M(T)/M(0)$, and the reduced mean hyperfine field, $b_{\rm hf} = B_{\rm hf}(T)/B_{\rm hf}(0)$, follow the same temperature dependence [11]. The temperature dependence of $M(T)$ can be determined by solving the equation $M(T) = M(0)B_J((M(T)/M(0))/(T/T_{\rm C}))$ based on a mean field theory for $T \leqslant T_{\rm C}$, where the function $B_J(x) = ((2J+1)/2J)\coth((2J+1)x/2J) - (1/2J)\coth(x/2J)$ is the *Brillouin function (BF)* and the calculated $M(T)$ is referred to as a BF relation [12]. The mean field theory predicts the magnetic transition at $T_{\rm C}$ to be second order. If the temperature dependence of $M(T)$ obviously deviates from the BF relation near $T_{\rm C}$, the magnetic transition should be first order. The $LaFe_{13-x}Si_x$ compounds display critical behaviour as isotropic Heisenberg ferromagnets [5] and $B_{\rm hf}(T)$ could be thus expressed by a BF with $J = \frac{1}{2}$, as

$$B_{\rm hf}(T) = B_{\rm hf}(0)B_{1/2}(x) \tag{1}$$

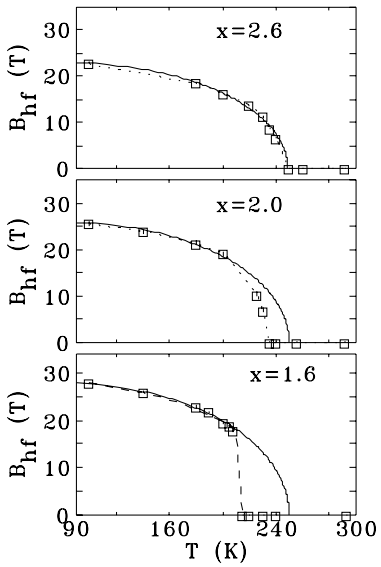

Figure 4. Temperature dependence of the hyperfine field, $B_{\rm hf}$, of $LaFe_{13-x}Si_x$ compounds. The solid curve is calculated using mean field theory (equation (1)). The dashed curve through the experimental data points is a guide to the eye.

Table 2. Curie temperatures for $LaFe_{13-x}Si_x$ compounds.

x	$T_{\rm C}^{\chi}$ (K)	$T_{\rm C}^{B_{\rm hf}}$ (K)	$T_{\rm C}^{\rm BF}$ (K)
1.6	203 ± 1	202 ± 3	250 ± 5
2.0	235 ± 1	235 ± 3	250 ± 8
2.6	249 ± 1	250 ± 3	250 ± 5

where

$$B_{1/2}(x) = 2\coth(2x) - \coth(x), \qquad x = b_{\rm hf}/t, \qquad t = T/T_{\rm C}.$$

$B_{\rm hf}(T)$ for $LaFe_{13-x}Si_x$ compounds were fitted using a standard least squares method and equation (1). The results are shown in figure 4. For each pair of input values of $B_{\rm hf}(0)$ and $T_{\rm C}$, a group of data of $B_{\rm hf}(T)$ at different temperatures, T, can be obtained by solving equation (1) numerically. Two fitted parameters of $B_{\rm hf}(0)$ and $T_{\rm C}^{\rm BF}$ can be derived from the calculated $B_{\rm hf}(T)$ and corresponding experimental data by a standard least squares method. The mean field theory may fail as the temperature approaches $T_{\rm C}$. In the fitting process, the measured data far below $T_{\rm C}$ are used first and the other points are gradually added unless they significantly increase the error. The uncertainties for fitted parameters of $B_{\rm hf}(0)$ and $T_{\rm C}^{\rm BF}$ depend on the number of points used in the fitting process and their measurement errors (table 2).

$B_{\rm hf}(T)$ for $LaFe_{10.4}Si_{2.6}$ can be fitted very well using the BF relation. However, with increasing temperature, $B_{\rm hf}(T)$ changes more sharply than that predicted by the BF relation near $T_{\rm C}$ for the $LaFe_{11.4}Si_{1.6}$ compound. This behaviour confirmed that a first order F–P transition occurs in $LaFe_{11.4}Si_{1.6}$ and a second order one in the $LaFe_{10.4}Si_{2.6}$ compound, in agreement with the magnetic measurement results [13]. This is also the main reason that $LaFe_{11.4}Si_{1.6}$ has a much larger magnetic entropy change near $T_{\rm C}$. The temperature dependence of $B_{\rm hf}(T)$ for $LaFe_{11.4}Si_2$ deviates from the BF relation, but not as sharply as that for the $LaFe_{11.4}Si_{1.6}$ compound, indicating a weak first order magnetic transition at $T_{\rm C}$. The results

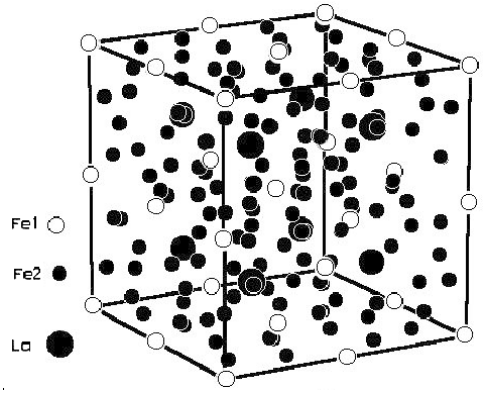

Figure 5. Crystallographic unit cell for $LaFe_{13-x}Si_x$ compounds. The sites of La (8a), Fe_1 (8b) and Fe_2 (96i) are occupied by the atoms of La, Fe and Fe (and/or Si), respectively.

are also in agreement with the fact that the AC magnetic susceptibility change becomes much sharper near T_C with decreasing Si content (figure 2).

The fitted values of magnetic transition temperature T_C^{BF} are listed in table 2 together with the $T_C^{B_{hf}}$ values determined from the appearance of the doublet and/or the disappearance of the sextet. Transition temperatures, T_C^{χ}, obtained from χ_{ac} measurements are identical, within error, to $T_C^{B_{hf}}$. However, for the alloys with $x = 1.6$ and 2.0, $T_C^{B_{hf}}$ is smaller than T_C^{BF} due to the fact that $B_{hf}(T)$ changes more sharply than predicted by the BF relation near T_C.

It is interesting to note that the fitted magnetic transition temperature, T_C^{BF}, is the same (about 250 K) for all three compounds. The compounds of $La(Fe, Al)_{13}$ with the $NaZn_{13}$ structure also have a maximum Curie temperature of 250 K [14].

3.3. Relationship between structure and magnetic phase transition

In order to understand the relationship between structure and magnetic properties, a Wigner–Seitz cell analysis was done on all the compounds. The Wigner–Seitz cell reflects the site symmetry and volume as well as the number and type of near neighbours and the interatomic distances [15]. The Wigner–Seitz cell calculation was performed following the method described in [15].

Figure 5 displays the unit cell for the $LaFe_{13-x}Si_x$ compound. As stated above, the sites of La (8a), Fe_1 (8b) and Fe_2 (96i) are occupied by the atoms of La, Fe and Fe (and/or Si), respectively. The interatomic distances between the near neighbours, La–Fe_2, Fe_1–Fe_2 and Fe_2–Fe_2, are directly derived from Wigner–Seitz calculations (figure 6). The interatomic distances are determined by the unit cell dimension and the atomic fractional coordinates. In addition, the average Fe_2–Fe_2 distance is calculated by the weighted average of all Fe_2–Fe_2 interatomic distances (figure 6). Similarly, the weighted average of Fe–Fe distances is obtained using all Fe_1–Fe_2 and Fe_2–Fe_2 interatomic distances (figure 7).

The Wigner–Seitz analysis shows that the La atom (8a) has 24 near neighbours of Fe_2 (Fe or Si) atoms (96i), but no near neighbours of Fe_1 atoms (8b) (figure 5). With increasing Si content, the La–Fe_2 distance decreases, indicating strengthening the La–Fe_2 bond (figure 6). An estimate for the affinity of one element to the other can be obtained from the empirical calculation of the enthalpy of mixing as proposed by Miedema [16]. The enthalpy of mixing gives a measure of the relative bond strengths of La–(Si, Fe) and Fe–Si. The enthalpy of mixing

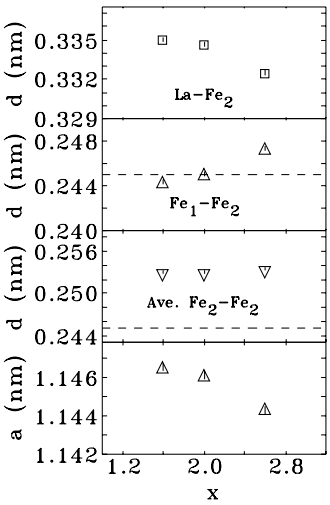

Figure 6. Interatomic distances, d, derived from the Wigner–Seitz calculation and lattice parameter, a, in $LaFe_{13-x}Si_x$ compounds. The average Fe_2–Fe_2 distance means the weighted average of all Fe_2–Fe_2 nearest-neighbour distances. The dashed line indicates the position of the critical Fe–Fe distance (2.45 Å).

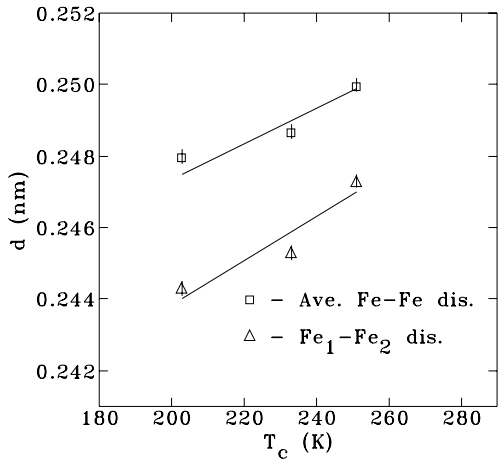

Figure 7. Relationship between T_C and Fe–Fe interatomic distance in $LaFe_{13-x}Si_x$ compounds. The average Fe–Fe distance means the weighted average value of all Fe_1–Fe_2 and Fe_2–Fe_2 nearest-neighbour distances.

for La–Si (-58 kJ mol^{-1}) is much larger and more negative than that for Fe–Si (-34 kJ mol^{-1}). However, the enthalpy of mixing for La–Fe is positive (+19 kJ mol^{-1}). It is for just this reason that the binary compound, $LaFe_{13}$, does not exist, while $LaFe_{13-x}Si_x$ compounds are stable with $x \geqslant 1.3$. This also explains why the Si atoms only enter the 96i sites and the La–Fe_2 bond length decreases with increasing Si content.

The strong La–Si bonds play an important role in the structure of $LaFe_{13-x}Si_x$ compounds. The La atom and its near neighbours ($24Fe_2$) constitute a strong structural cluster $La(Fe, Si)_{24}$, which determines the stability of the cubic $NaZn_{13}$ structure. The replacement of some La–Fe pairs by La–Si pairs can stabilize this cluster and thus maintain the $NaZn_{13}$ structure. However,

a further increase in Si content will destroy the cubic structure. As mentioned above, the Si and Fe atoms are randomly distributed at 96i sites with the same fractional coordinates in the cubic $LaFe_{13-x}Si_x$ compound. However, the large difference in affinity between La–Si and La–Fe pairs will introduce changes in the interatomic distances of the pairs and the structural stability of the cluster will be lowered. Indeed, the compound of $LaFe_9Si_4$ possesses a tetragonal structure which can be derived from the $NaZn_{13}$ structure [17]. In this compound, the 96i site is split into three inequivalent sites, i.e., 16l(1), 16k and 16l(2). Si atoms occupy the 16l(2) positions. The tetragonal structure corresponds to an ordered occupation of Si atoms and possesses a paramagnetic ground state [18].

The Fe_2 atom has nine near neighbours of Fe_2 in addition to two neighbours of La and one neighbour of Fe_1. The average interatomic distance of Fe_2–Fe_2 is slightly larger than that of Fe_1–Fe_2 and remains almost unchanged (about 2.53 Å) with increasing Si content (figure 6).

It is interesting to note that the Fe_1–Fe_2 distance is increased while the lattice constant is decreased with increasing Si content (figure 6). The Fe_1 is surrounded by 12 near neighbours of Fe_2 (Fe or Si) atoms at the vertices of a regular icosahedron. The icosahedral $(Fe_1–Fe_2)_{13}$ can be considered as a superatom (figure 5). In this picture, the basis for the cubic $NaZn_{13}$ type structure can be described as a La atom and a $(Fe_1–Fe_2)_{13}$ superatom. The La is nonmagnetic and the magnetic contribution is mainly from the superatoms. According to Givord and Lemaire [19], there are two Fe–Fe exchange interactions in R_2Fe_{17} compounds, positive and negative. When the separation of the Fe–Fe pair is smaller than 2.45 Å the exchange interaction is negative while the interaction is positive at larger Fe–Fe distances. For the $LaFe_{13-x}Si_x$ compounds, the radius of the $(Fe_1–Fe_2)_{13}$ icosahedron, i.e. Fe_1–Fe_2 atomic distance, is 2.443, 2.450 and 2.473 Å for $x = 1.6$, 2.0 and 2.6, respectively. On the other hand, the average Fe_2–Fe_2 distance remains almost unchanged (about 2.53 Å) and is larger than the critical distance of 2.45 Å in $LaFe_{13-x}Si_x$ compounds. The Fe_1–Fe_2 distance plays the critical role in the exchange interaction and T_C in $LaFe_{13-x}Si_x$ compounds. With increasing Si content, the Fe_1–Fe_2 distance increases, which enhances the positive exchange interaction in the $(Fe_1–Fe_2)_{13}$ cluster and thus increases T_C. Figure 7 shows the relationship between the Fe–Fe interatomic distance and T_C in $LaFe_{13-x}Si_x$ compounds. The figure clearly shows the good correlation between T_C and the Fe_1–Fe_2 distance and the weighted average of Fe–Fe distance. Similar results have been reported in other R–Fe compounds [20].

The nature of the P–F magnetic transition at T_C in $LaFe_{13-x}Si_x$ compounds is intimately related to the coupling between the lattice and magnetism. The Fe_1–Fe_2 distance for the compounds with $x = 1.6$ and 2.0 is near the critical boundary of negative and positive exchange interactions while that for $x = 2.6$ is larger than 2.45 Å. However, the large magnetovolume effect, resulting from the coupling between the lattice and magnetism, can increase the Fe_1–Fe_2 distance markedly and enhance the positive interaction in the superatom $(Fe_1–Fe_2)_{13}$. In fact, $LaFe_{11.4}Si_{1.6}$ has a large negative lattice expansion up to 0.4% between the paramagnetic and ferromagnetic states near T_C, but that for $LaFe_{10.4}Si_{2.6}$ is less than 0.05% [3]. This conforms to the fact that $LaFe_{11.4}Si_{1.6}$ shows a strong first order magnetic transition at T_C while the transition is second order for the $LaFe_{10.4}Si_{2.6}$ compound. Clearly, the different order of the magnetic transition for compounds with different Si content originates from the variation of the La–(Fe, Si) and the average Fe–Fe near neighbour distances, particularly that of Fe_1–Fe_2.

4. Conclusion

Room temperature XRD analysis indicates the lattice constant decreases with increasing Si content. Wigner–Seitz cell calculations show that the La (8a)–Fe_2 (96i) interatomic distance decreases while that of Fe_1 (8b)–Fe_2 (96i) increases with Si content. The average Fe_2–Fe_2

distance remains almost unchanged and the average Fe–Fe distance increases with Si content. The replacement of some La–Fe pairs by La–Si pairs can improve the structural stability of the cubic $LaFe_{13-x}Si_x$ compound according to Miedema's model. The larger Fe–Fe atomic distance in $LaFe_{13-x}Si_x$ compounds enhances the positive exchange interaction, which conforms to the fact that the T_C increases with Si content. Analysis of the temperature dependence of the hyperfine fields indicates that a first order magnetic transition occurs in the compounds with $x = 1.6$ and 2.0 and a second order one in the $LaFe_{10.4}Si_{2.6}$ compound.

The nature of the magnetic transition for $LaFe_{13-x}Si_x$ compounds at T_C is intimately related to the magnetovolume effect. The different order of the magnetic transition for compounds with different Si content originates from the spatial distribution of the Si atoms and related variation of interatomic distance of La–(Fe, Si) and Fe–Fe in the $NaZn_{13}$ cubic structure.

References

[1] Pecharsky V K and Gschneidner K A 1997 *Appl. Phys. Lett.* **70** 3299
[2] Guo Z B, Zhang J R, Huang H, Ding W P and Du Y W 1997 *Appl. Phys. Lett.* **70** 904
[3] Hu F X, Shen B G, Sun J R, Cheng Z H, Rao G H and Zhang X X 2001 *Appl. Phys. Lett.* **78** 3675
[4] Tegus O, Bruck E, Buschow K J H and de Boer F R 2002 *Nature* **415** 150
[5] Palstral T T M, Mydosh J A, Nieuwenhuys G J, van der Kraan A M and Buschow K H J 1983 *J. Magn. Magn. Mater.* **36** 290
[6] Wen G H, Zheng R K, Zhang X X, Wang W H, Chen J L and Wu G H 2002 *J. Appl. Phys.* **91** 8537
[7] Rietveld H M 1967 *Acta Crystallogr.* **22** 151
[8] Rodriguez-Carvajal J 2000 *Program FullProf 2000* Laboratoire Leon Brillouin
[9] Villars P and Calvert L D 1986 *Pearson's Handbook of Crystallographic Data for Intermetallic Phase* (Metal Park, OH: American Society of Metals) p 2646
[10] Zhao Y M, Liang J K, Rao G H, Tang W H and Guo Y H 1997 *J. Phys.: Condens. Matter* **9** 7463
[11] Greenwood N N and Gibb T C 1971 *Mössbauer Spectroscopy* (London: Chapman and Hall) p 63
[12] Kittel C 1976 *Introduction to Solid State Physics* 5th edn (New York: Wiley) p 440, 463
[13] Fujita A, Fujieda S and Fukamichi K 2001 *Phys. Rev.* B **65** 014410
[14] Palstral T T M, Nieuwenhuys G J, Mydosh J A and Buschow K J H 1984 *J. Appl. Phys.* **55** 236
[15] Koch E and Fischer W 1996 *Z. Kristallogr.* **211** 251
[16] Miedema A R, Boom F R and de Boer R 1992 *Physica* B **182** 1
[17] Tang W H, Liang J K, Chen X L and Rao G H 1994 *J. Appl. Phys.* **76** 4095
[18] Tang W H, Liang J K, Rao G H and Yan X H 1994 *Phys. Status Solidi* a **141** 217
[19] Givord D and Lemaire R 1974 *IEEE Trans. Magn.* **10** 109
[20] Mara Singhe G K, Ezekwenana P C, James W J, Hu Z and Yelon W B 1997 *J. Appl. Phys.* **81** 5103